Sheath boundary conditions for plasma fluid models

J. Loizu, P. Ricci, C. Theiler, I. Furno and A. Fasoli

Ecole Polytechnique Fédérale de Lausanne (EPFL), Centre de Recherches en Physique des Plasmas, Association Euratom-Confédération Suisse, CH-1015 Lausanne, Switzerland

1. Introduction and Motivation

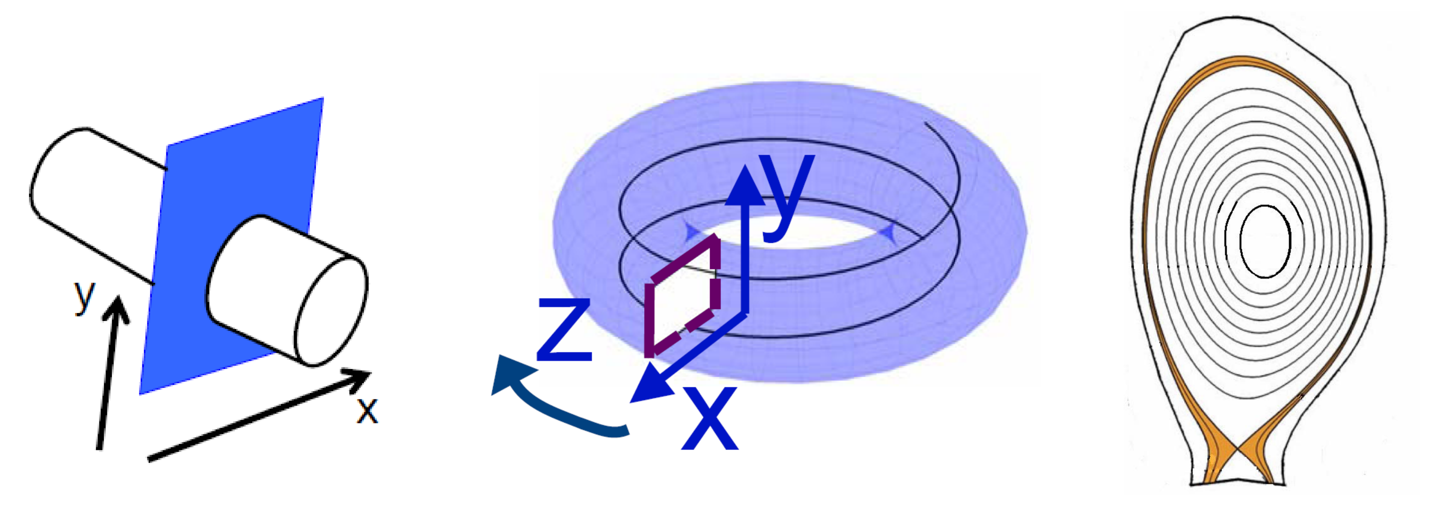

(a) (b) (c)

When a plasma interacts with an absorbing wall, a non-neutral sheath forms. Plasma properties at the sheath edge determine:

- The boundary conditions for any model assuming quasi-neutrality
- The particle and energy fluxes at the solid surface

In basic plasma physics experiments, the whole device displays open magnetic field lines, and most of the plasma is lost in the regions of the vessel where these lines end (**a**, **b**). In the SOL of tokamaks, plasma circulates with losses at the divertors or limiters (**c**).

2. Boundary conditions for Braginskii equations

A particular example of the simulation effort towards the understanding of edge turbulence is the Global Braginskii Solver (GBS), a 3D fluid code based on the drift-reduced Braginskii equations [1], with cold ions and quasi-neutral plasma,

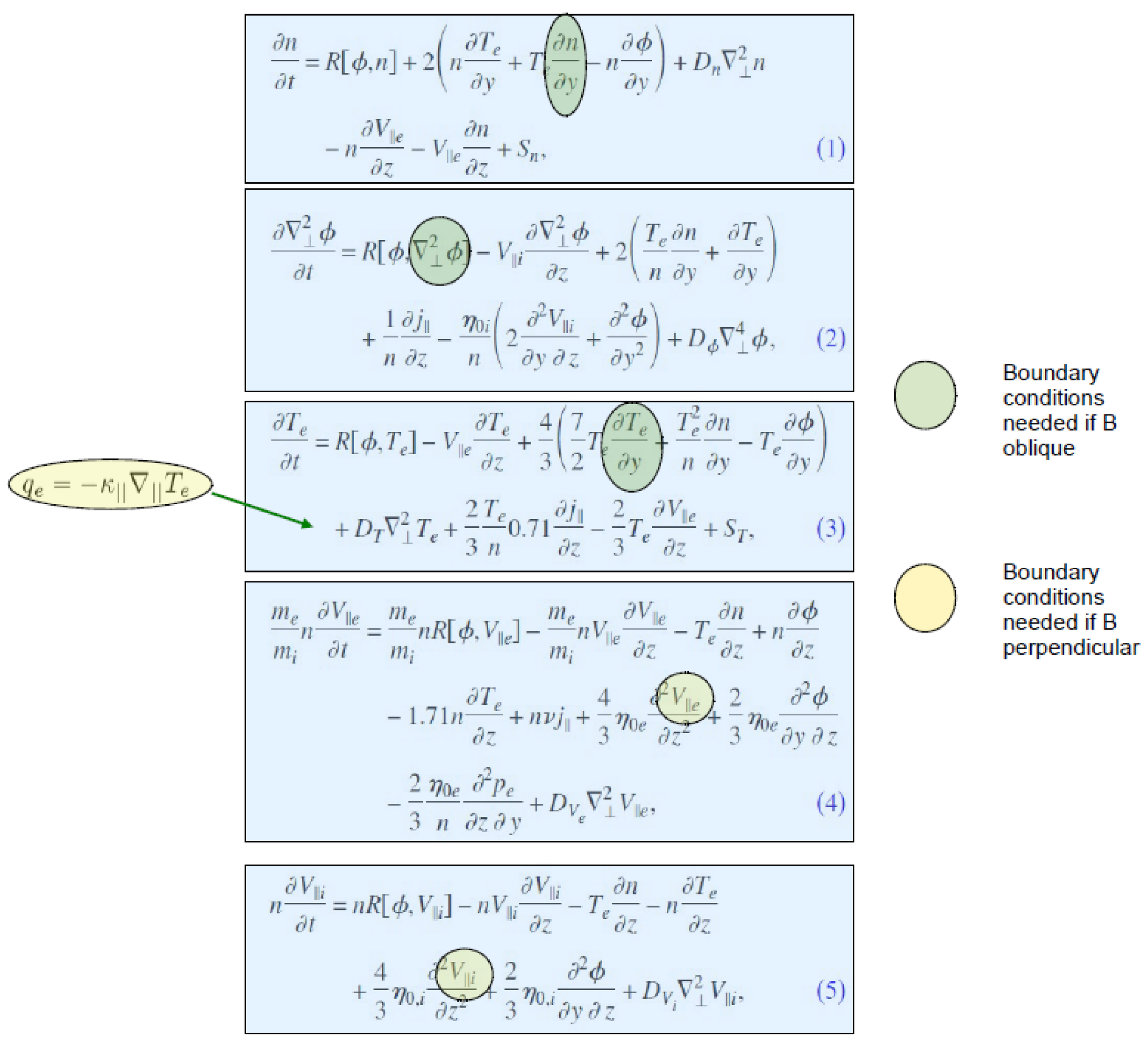

It has been used to simulate the full TORPEX device [2] (**b**), identifying the nature of the instablities in the different turbulent regimes. However, **the sheath boundary conditions strongly affect several properties of the plasma**, e.g. the steady state profiles.

3. Electrostatic Sheath PIC code (ESS)

A fully kinetic, 1d3v, electrostatic PIC code has been developed to investigate how the sheath forms and what are the plasma properties at the sheath entrance.

The code evolves self-consistently a plasma bound in between two conducting (absorbing) walls, by solving the Vlasov-Poisson system:

$$\frac{\partial f_s}{\partial t} + \mathbf{v}\cdot\frac{\partial f_s}{\partial \mathbf{x}} + \frac{q_s}{m_s}(\mathbf{E} + \mathbf{v}\times\mathbf{B_0})\cdot\frac{\partial f_s}{\partial \mathbf{v}} = \left(\frac{\partial f_s}{\partial t}\right)_{source}$$

$$\nabla^2\phi = -\frac{e}{\epsilon_0}\int (f_i(\mathbf{x},\mathbf{v}) - f_e(\mathbf{x},\mathbf{v}))d^3v$$

Particles are moved according to the Lorentz force by using the Boris algorithm. The electric field is self-consistently updated with Poisson's equation, and the magnetic field is constant and tilted.

Collisions between electrons are implemented according to a Fokker Planck collision operator [3], conserving energy and momentum.

Physical parameters of the system:

- Mass ratio $\mu = m_i/m_e$
- Temperature ratio $\tau = T_i/T_e$
- Angle of incidence α between **B** and the wall
- Electron mean free path λ_{mfp}
- Current driven into the system $J = \Gamma_i - \Gamma_e$

Numerical parameters of the system:

- System size $L \gg \lambda_D$
- Source shape and strength $S(x, v)$
- $\Delta x \lesssim \lambda_D$
- $\Delta t \lesssim \omega_{pe}^{-1}, \omega_{ce}^{-1}$
- Computational particles N_p injected per Δt

The code is parallelized with the Message Passing Interface (MPI) library, by using the domain decomposition method. It typically runs on 8 processors for several hours.

4. Numerical results (case $\alpha = \pi/2$)

The steady-state macroscopic profiles and the electron velocity distribution function $f_e(x, v_x)$ are shown, for the case $\alpha = \pi/2$, $\mu = 100$, $\tau = 0.005$, $\lambda_{mfp} = 300\lambda_D$, and $J = 0$.

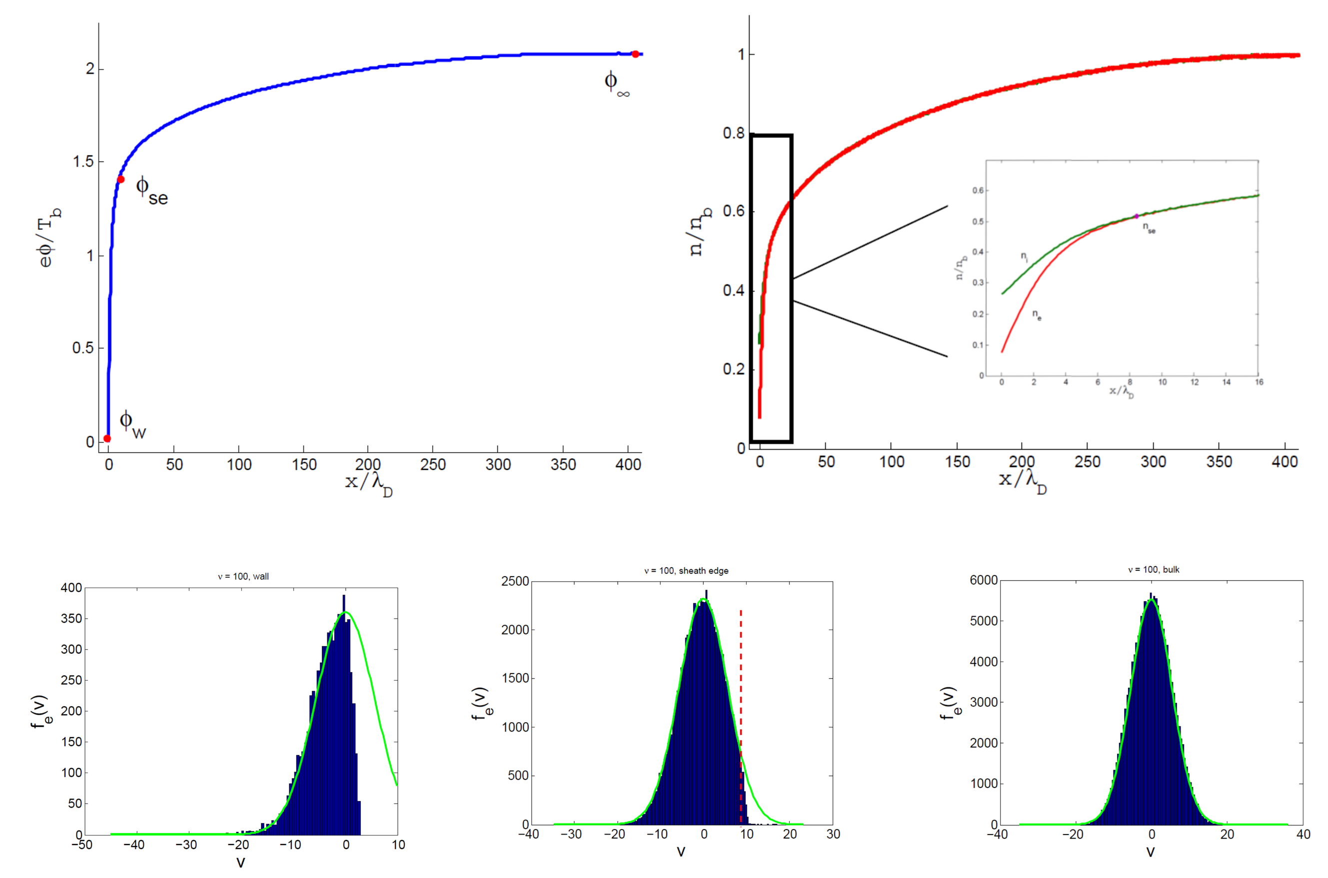

5. Analytical description of the sheath edge

- By defining the quantity $\eta(x) = e\phi(x)/T_b$, where T_b is the bulk temperature in the main plasma,

$$f_e(v_x,\eta) = \frac{1}{I(\eta)\sqrt{2\pi v_{thb}^2}}\exp\left(-\frac{v_x^2}{2v_{thb}^2}\right) \quad \text{for} \quad v_x < v_{cut}(\eta)$$

with the electron fluid velocity, $V_e = \langle v_x\rangle$, and heat flux, $q_e = \frac{1}{2}n_e m_e\langle(v_x - V_e)^3\rangle$, given by

$$\boxed{V_e = \frac{c_{sb}}{I(\eta)}\exp(\Lambda - \eta)} \qquad (1)$$

$$\boxed{q_e = \frac{n_e m_e v_{thb}^3}{\sqrt{2\pi}I(\eta)}\left[e^{-\eta}\left(\eta - \frac{1}{2}\right) + \frac{3}{2}\sqrt{\frac{\eta}{\pi}}\frac{e^{-2\eta}}{I(\eta)} + \frac{e^{-3\eta}}{2\pi I^2(\eta)}\right]} \qquad (2)$$

where $v_{thb} = \sqrt{T_b/m_e}$, $v_{cut}(\eta) = \sqrt{2\eta}v_{thb}$, $I(\eta) = \left[1 + \mathrm{erf}(\sqrt{\eta})\right]/2$, $c_{sb} = \sqrt{T_b/m_i}$ and $\Lambda = \log\sqrt{\mu/2\pi}$.

- The first two moments of the Vlasov equation for ions and the first moment for electrons (continuity and momentum equations), in steady state conditions, are

$$n_i\frac{\partial V_i}{\partial x} + V_i\frac{\partial n_i}{\partial x} = S_{pi}$$
$$n_e\frac{\partial V_e}{\partial x} + V_e\frac{\partial n_e}{\partial x} = S_{pe}$$
$$m_i n_i V_i\frac{\partial V_i}{\partial x} = -en_i\frac{\partial \phi}{\partial x} + S_{mi}.$$

- By imposing the presheath condition $n_i = n_e$, and writing the term $\partial_x V_e$ as $\partial_\phi V_e \partial_x\phi$, we are left with a matrix system $\mathbf{M}\vec{X} = \vec{S}$, where

$$\mathbf{M} = \begin{pmatrix} V_i & n & 0 \\ V_e & 0 & n\partial_\phi V_e \\ 0 & m_i V_i & e \end{pmatrix}, \qquad \vec{X} = \begin{pmatrix} \partial_x n \\ \partial_x V_i \\ \partial_x \phi \end{pmatrix}, \qquad \vec{S} = \begin{pmatrix} S_{pi} \\ S_{pe} \\ S_{mi} \end{pmatrix}.$$

- At the sheath edge, gradients become very steep, i.e. $|M_{\alpha\beta}X_\beta| \gg |S_\alpha|$ for all α, β such that $M_{\alpha\beta} \neq 0$. This leads to $\mathbf{M}\vec{X} \simeq 0$ at the sheath edge, and non-zero gradients impose $\det(\mathbf{M}) = 0$, giving

$$\boxed{V_i = c_{sb}\sqrt{\frac{1}{1+\kappa}}} \qquad (3)$$

where

$$\kappa = \frac{e^{-\eta_{se}}}{2\sqrt{\pi\eta_{se}}I(\eta_{se})}$$

6. Comparison

The theoretical predictions for $V_{\parallel i}$, $V_{\parallel e}$, and q_e at the sheath edge are compared with the numerical results, and plotted as a function of the sheath edge potential η_{se}. The sheath edge location is found according to Eq. (3).

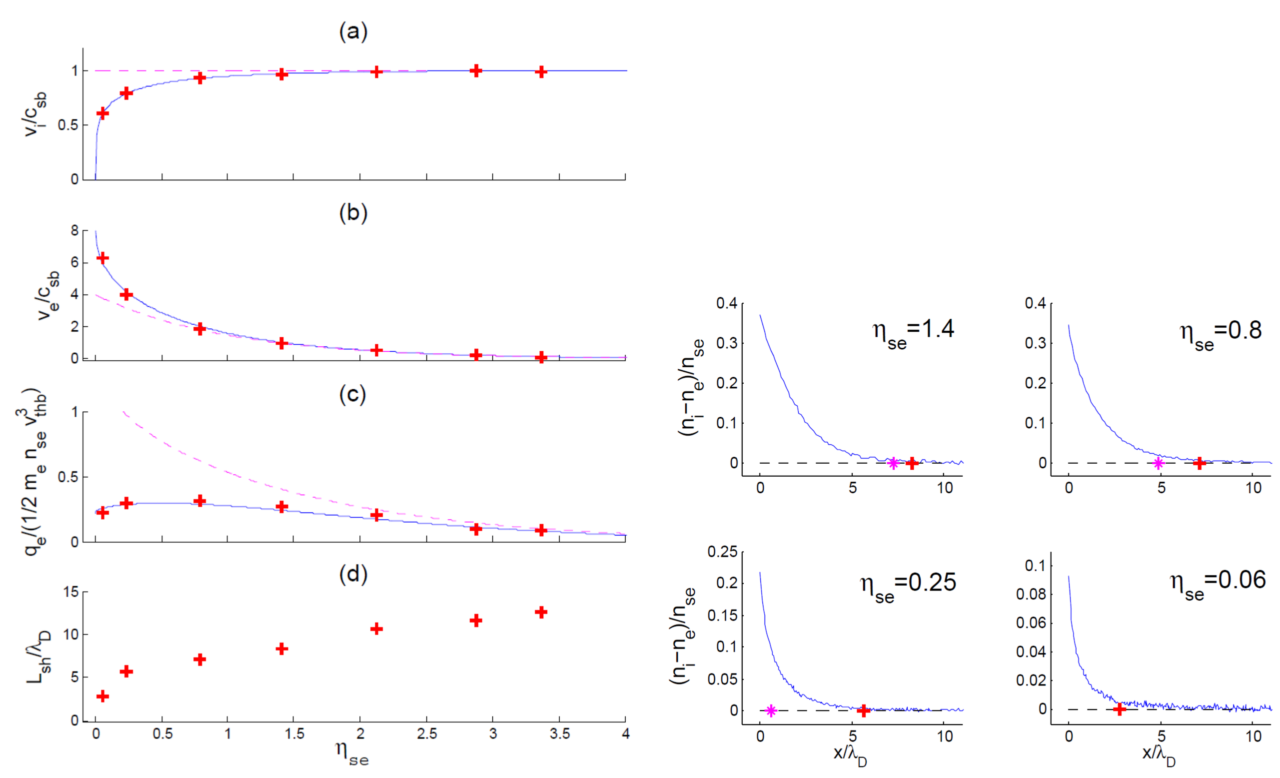

In the case of predominant electron current ($J < 0$ or $\eta_{se} < \Lambda$), the **Bohm criterion** [4], $V_i = c_s$, **is not able to describe the transition to the non-neutral region** (magenta stars), while Eq. (3) remains coherent (red crosses) no matter what the plasma current is. This result can be relevant wherever there are transient electron currents to the wall, e.g. in the modeling of ELMs [5].

An **experimental verification of this effect** could be carried out by using an emissive probe to inject an electron current in the plasma. The ion velocity, measured by means of a Mach probe or using LIF, should be strongly reduced under such current. The effect should be noticable for electron currents $I_e \sim 10enc_s$.

7. Further work

The boundary conditions needed in the case $\alpha = \pi/2$ are given by equations (1)-(3). Simulations are being performed with $\alpha < \pi/2$ in order to extract a complete analytical set of local boundary conditions.

References :

[1] P. Ricci and B. N. Rogers, Turbulence phase space in Simple Magnetized Toroidal Plasmas, Phys. Rev. Lett. 104, 145001 (2010)

[2] A. Fasoli, B. Labit, M. McGrath et al, Electrostatic Turbulence and Transport in a Simple Magnetized Plasma , Phys. Plasmas, 13, 055902, (2006)

[3] T. Takizuka, J. Comp. Phys. 25, 205-219 (1977)

[4] D. Bohm, *The Characteristics of Electrical Discharges in Magnetic Fields*, ch 3, p. 77 (1949)

[5] T.D. Rognlien et al., J. Nucl. Mater. 313-316, 1000-1004 (2003)